Available online at www.sciencedirect.com
ScienceDirect
Bioorganic Chemistry 36 (2008) 77–84
BIOORGANIC CHEMISTRY
www.elsevier.com/locate/bioorg

Crosslinking of nucleotide excision repair proteins with DNA containing photoreactive damages

Ekaterina A. Maltseva [a,1], Nadejda I. Rechkunova [a,1], Irina O. Petruseva [a], Wim Vermeulen [b], Orlando D. Schärer [c], Olga I. Lavrik [a,*]

[a] *Laboratory of Bioorganic Chemistry of Enzymes, Institute of Chemical Biology and Fundamental Medicine, Lavrentiev Av. 8, 630090 Novosibirsk, Russia*
[b] *Department of Cell Biology and Genetics, University of Erasmus Medical Center Rotterdam, Dr. Molenwaterplein 50, 3015 GE Rotterdam, The Netherlands*
[c] *Department of Pharmacological Sciences, SUNY Stony Brook, Stony Brook, NY 11794-3400, USA*

Received 12 September 2007
Available online 11 January 2008

Abstract

Photoreactive DNA duplexes mimicking substrates of nucleotide excision repair (NER) system were used to analyze the interaction of XPC–HR23B, RPA, and XPA with damaged DNA. Photoreactive groups in one strand of DNA duplex (arylazido-dCMP or 4-thio-dUMP) were combined with anthracenyl-dCMP residue at the opposite strand to analyze contacts of NER factors with damaged and undamaged strands. Crosslinking of XPC–HR23B complex with photoreactive 48-mers results in modification of XPC subunit. XPC–HR23B did not crosslink with DNA duplex bearing bulky residues in both strands while this modification does not prevent interaction of DNA with XPA. The data on crosslinking of XPA and RPA with photoreactive DNA duplexes containing bulky group in one of the strands are in favor of XPA preference to interact with the damaged strand and RPA preference for the undamaged strand. The results support the understanding and set the stage for dynamically oriented experiments of how the pre-incision complex is formed in the early stage of NER.
© 2007 Elsevier Inc. All rights reserved.

Keywords: Nucleotide excision repair; XPC–HR23B; XPA; Replication protein A; Photoaffinity labeling; Model DNA duplexes imitating NER substrates

1. Introduction

Cellular DNA is continuously exposed to chemical reactions with numerous endogenous and exogenous agents. The resulting alterations in DNA can provoke cellular dysfunctions, such as genetic instability, mutagenesis or cell death. Several DNA repair pathways counteract these adverse effects of damaging agents. One of the most versatile mammalian repair systems is nucleotide excision repair (NER), which is able to remove a wide range of lesions from DNA, including those formed by solar UV light, various environmental mutagens and certain chemotherapeutic agents and to function in protecting humans against cancer. NER engages over 30 polypeptides involved in the following stages: damage recognition, opening of the DNA around the lesion, dual strand incision and removal of the damaged region, synthesis to fill in the excised strand, and ligation [1–4]. In eukaryotic cells, different NER pathways have been identified for repair of actively transcribed genes (transcription-coupled repair, TCR)

Abbreviations: NER, nucleotide excision repair; RPA, replication protein A; XPA, xeroderma pigmentosum group A protein; XPC, xeroderma pigmentosum group C protein; HR23B, homolog B of Rad23; FAP-dCTP, exo-N-{2-[N-(4-azido-2,5-difluoro-3-chloropyridine-6-yl)-3-aminopropionyl]-aminoethyl}-2′-deoxycytidinetriphosphate; S4-dUTP, 4-(thio)-2′-deoxyuridinetriphosphate; Antr-dCTP, exo-N-[2-(4-antracenyl)-ethyl]-2′-deoxycytidinetriphosphate; GGR, global genome repair; EMSA, electrophoretic mobility shift assay.

* Corresponding author. Fax: +7 383 333 3677.
E-mail addresses: w.vermeulen@erasmusmc.nl (W. Vermeulen), orlando@pharm.stonybrook.edu (O.D. Schärer), lavrik@niboch.nsc.ru (O.I. Lavrik).

[1] These authors contributed equally to this work.

0045-2068/$ - see front matter © 2007 Elsevier Inc. All rights reserved.
doi:10.1016/j.bioorg.2007.11.004

and for repair of non-transcribed genomic DNA (global genome repair, GGR) [5]. While for both processes a similar set of proteins seems to be involved in the later steps, clear differences exist in early stages of damage recognition and organization of the pre-incision complex. A two-step model of damage recognition in GGR has been proposed to function in repair of helix distortion, an initial recognition of the distortion and a subsequent verification of the damage [6,7]. According to the current model, initial recognition in GGR is performed by the hetero-trimeric complex XPC–HR23B–Cen2 [8–10]. XPC bound to lesions recruits the DNA repair/transcription complex TFIIH to the site of the lesion [11], and partial opening of the DNA helix is mediated by the XPD and XPB helicases of TFIIH [12]. The fully opened DNA structure in the pre-incision complex is obtained after the recruitment of XPG, RPA and XPA. The coordinated assembly of the NER pre-incision complexes is guided by multiple protein interactions [13]. The overall NER mechanism is fairly well understood, however, details of the damage recognition and NER processing remain unknown. Although it is widely accepted that XPC–HR23B is the first factor responsible for the assembly of the NER reaction complex, its precise role in the damage recognition process remains unknown. Moreover, the implications of RPA and XPA are not understood as well as their participation in primary damage recognition is not excluded completely. A model of the random order assembly proposes cooperative damage recognition by RPA, XPA, and XPC followed by kinetic proofreading by the TFIIH complex [14,15].

Bulky photoreactive dNMP analogs introduced into DNA constitute targets for the bacterial NER system, and they are recognized and processed by UvrABC proteins [16]. Arylazido derivatives of both dCMP and dUMP when introduced into DNA are damages recognized by the mammalian NER system [17]. On that basis, DNA constructs containing bulky photoreactive substituents can be used as photoreactive intermediates of NER to investigate loading of protein factors on damaged DNA. The method of using photoreactive bulky nucleotide analogs is in particular applicable to study NER intermediates of low affinity that are formed during DNA repair.

In the present work, we studied the interaction of XPC–HR23B, RPA, and XPA with 48-mer DNA structures containing the arylazido group in the inner positions of single-stranded or double-stranded DNA. In particular, we have combined photoreactive arylazido or thio group in one of the strands of DNA duplex with bulky anthracene group in the opposite DNA strand to analyze contacts of XPC–HR23B, XPA, and RPA in cases of damage on one DNA strand and damages on both strands of the DNA duplex. This analysis contributes to the understanding of how these proteins are involved in nucleotide excision repair. The goal of the present investigation is the demonstration that binding of a DNA-damage site to NER recognition proteins can be followed by the method of photochemical crosslinking, and that the method allows to detect structural changes at the damage recognition complex. The results will set the first stage for dynamic studies following the course of the recognition and repair reactions.

2. Materials and methods

[γ-^{32}P] ATP (5000 Ci/mmol) was from the Laboratory of Biotechnology (Institute of Chemical Biology and Fundamental Medicine (ICBFM), Novosibirsk, Russia). T4 polynucleotide kinase and T4 DNA ligase were from Biosan (Russia). Reagents for electrophoresis and basic components of buffers were from Sigma (USA). Rainbow colored protein molecular mass markers were from Amersham. Photoreactive dCTP analog, exo-N-{2-[N-(4-azido-2,5-difluoro-3-chloropyridine-6-yl)-3-aminopropionyl]-aminoethyl}-2′-deoxycytidinetriphosphate (FAP-dCTP), was synthesized according to [18], 4-(thio)-2′-deoxyuridinetriphosphate (S4-dUTP) was synthesized and kindly gifted by Viktor Bogachev, anthracene substituted dCTP, exo-N-[2-(4-antracenyl)-ethyl]-2′-deoxycytidinetriphosphate (Antr-dCTP) was synthesized and kindly gifted by Igor Safronov. Oligonucleotides were synthesized in the ICBFM using an ASM-800 oligonucleotide synthesizer (BIOSSET, Russia). The sequences of the oligonucleotides used in the experiments were as follows:

T1 5′-GGAAGACCCTGACGTTGCCCAACTTAATCGCC-3′

T2 5′-GGAAGACCCTGACGTTACCCAACTTAATCGCC-3′

T3 5′-GGCGATTAAGTTGGGCAACGTCAGGGTCTTCC-3′

T45′-GTCGTTCGGAAGACCCTGACGTTGCCCAACTTAATCGCCGCTCCATAG-3′

P1 5′-CTATGGCGAGGCGATTAAGTTGGG-3′

P2 5′-pAACGTCAGGGTCTTCCGAACGAC-3′

P3 5′-GTCGTTCGGAAGACCCTGACGTTG-3′

P4 5′-pCCAACTTAATCGCCGCTCCATAG-3′

2.1. Protein purification

Recombinant human RPA was isolated from a strain of *Escherichia coli* according to [19]. Polyhistidine tagged hXPA was expressed in *E. coli* BL21(DE3)LysS using the expression vector pET15b-XPA and purified to homogeneity through nickel beads, gel filtration and heparin sepharose columns. Polyhistidine-tagged hHR23B was expressed in *E. coli* BL21(DE3)LysS using the expression vector pET24d and purified on nickel beads. His- and MBP-tagged XPC was expressed in Sf9 insect cells using the expression vector pFastBac1. The cells were lysed as described [20] and S3 fraction was combined with partially purified hHR23B. The correctly folded heterodimer was further purified on nickel beads followed with gel-filtration and heparin sepharose columns. Recombinant rat DNA polymerase β (β-pol) was purified according to [21].

2.2. Radioactive labeling of oligonucleotide primers

Oligodeoxynucleotide P1 was 5′-[^{32}P]-phosphorylated with T4 polynucleotide kinase as described [22]. Unreacted [γ ^{32}P] ATP was separated by passing the mixture over a MicroSpin™ G-25 column (Amersham Pharmacia Biotech, NJ) using the manufacturer's suggested protocol.

2.3. Primer–template annealing

Complementary oligodeoxynucleotides were annealed by heating a solution of indicated amounts in 10 mM Tris–HCl, pH 7.8, and 1 mM EDTA to 90 °C for 3 min, followed by slow cooling to room temperature. Duplex DNA substrates were analyzed by electrophoresis using a 15% native polyacrylamide gel. In all our experiments the percentage of duplex formation was >95%.

2.4. Elongation of primers by β-pol using dNTP analogs

Standard reaction mixtures (50 μl) contained 50 mM Tris–HCl, pH 8.6, 50 mM KCl, 5 mM $MgCl_2$, 5 μM [^{32}P]-labeled one nucleotide gapped DNA, 15 μM FAP-dCTP, S4-dUTP or Antr-dCTP and 5 μM β-pol. The reaction mixtures were incubated at 37 °C for 30 min to allow elongation of the primers. The primer elongation rate was analyzed using 0.5 μl aliquots which were added to 5 μl of 90% formamide, 50 mM EDTA, 0.1% xylene cyanole and 0.1% bromophenol blue. The resulting mixtures were heated for 3 min at 95 °C and products were analyzed by electrophoresis in denaturing PAGE followed by autoradiography [22]. In all our experiments the percentage of primer elongation was >95%.

2.5. Ligation of oligonucleotides by T4 DNA ligase

To ligate a nick resulting from gap filling reaction, mixtures contained 1 mM ATP and T4 DNA ligase at 1 u.a./μl (one unit is defined as the amount of enzyme achieving 50% ligation of λ DNA HindIII fragments/300 μg/ml 5′ DNA termini in 20 μl reaction mixture for 30 min at 16 °C). Reaction mixtures were incubated at 16 °C for 90 min and separated by denaturing PAGE. 48-mer oligonucleotides were isolated from gel and used in further experiments. Photoreactive single-stranded oligonucleotide used as ssDNA probe or was annealed to equal amounts of unmodified or anthracene-containing oligonucleotides to obtain photoreactive DNA duplexes.

2.6. Electrophoretic mobility shift assays

Indicated amounts of RPA and XPA were incubated in 20 μl reaction mixtures containing 20 mM Tris–HCl, pH 7.5, 50 mM NaCl, 2 mM $MgCl_2$, 10 μg BSA, and 10 nM [^{32}P]-labeled DNA at 37 °C for 20 min. Binding reaction mixtures were brought to a final concentration of 5% glycerol and 0.01% bromophenol blue and electrophoresed on 4% native polyacrylamide gel (acrylamide:bisacrylamide, 30:1) in TAE for 1.5 h at 10 V/cm and room temperature. The gels were dried, exposed to PhosphorImager (BioRad) and bands were quantitated using BioRad software Quantity One.

2.7. Photochemical crosslinking

Reaction mixtures (10 μl) contained 50 mM Tris–HCl, pH 8.0, 50 mM NaCl, 5 mM $MgCl_2$, 50 nM [^{32}P]-labeled DNA, 0.1 μg BSA and indicated amounts of XPC, XPA and/or RPA. The mixtures were incubated in micro-Eppendorf tubes for 15 min at 37 °C and then irradiated on ice from above with UV-light. The probes containing the arylazido group were irradiated for 5 min using UV-crosslinker Bio-Link (Vilber Lourmat) equipped with 312 nm lamps (6 × 8 W), those containing thio derivatives for 45 min using a 313–365 nm UV-filter and a Lomo VIO-1 UV-crosslinker system (St. Petersburg, Russia) equipped with a high pressure mercury light source. Crosslinking was terminated by adding Laemmli loading buffer and heating for 5 min at 100 °C. The crosslinked protein–DNA samples were separated by 12% SDS–PAGE [23]. Gels were dried and subjected to overnight autoradiography using a PhosphorImager (BioRad) screen.

2.8. Preparation of DNA substrates

Photoreactive oligonucleotides were synthesized using the following protocol: P2 and 5′-^{32}P phosphorylated P1 primers were annealed to T1 or T2 template at a ratio of 2:1:1 to produce one nucleotide gapped DNA. The gap was filled by DNA polymerase β using photoreactive dCTP analog FAP-dCTP or S4-dUTP as substrates in primer elongation, and the resulting nick was ligated by T4 DNA ligase. FAP-dCMP incorporated into DNA imitated DNA damage recognized and processed by the mammalian NER system [17]. S4-dUTP was used to produce photoreactive oligonucleotide mimicking undamaged DNA strand. Because S4-dUMP is not bulky, it does not give rise to DNA distortion. An identical protocol was applied to synthesize Antr-dCMP containing oligonucleotide using P3 and P4 primers, T3 as template and anthracenyl derivative of dCTP. This residue was used as a bulky substituent despite its processing by NER system was not analyzed yet. Reaction mixtures were subjected to denaturing PAAG electrophoresis and 48-mer ligation products were isolated from gel. Photoreactive oligonucleotides were used as ssDNA probes or annealed with equimolar amounts of complementary oligonucleotide T4 or its derivative containing the Antr-dCMP residue. A scheme for the synthesis of photoreactive oligonucleotides and structures of base-substituted dCTP analogs and DNAs are presented in Scheme 1.

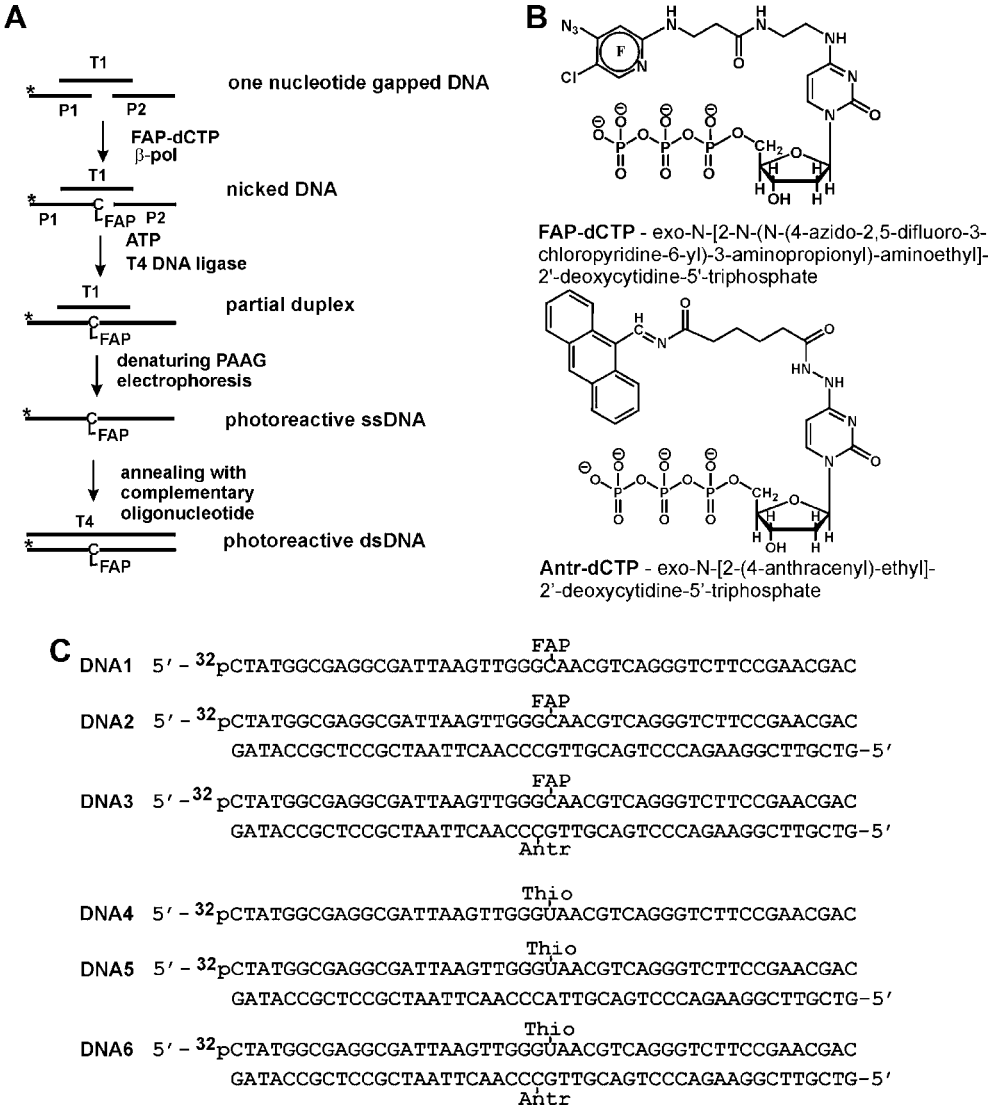

Scheme 1. DNA substrates used. (A) Scheme of enzymatic synthesis of photoreactive 48-mer oligonucleotide. P2 and 5′-^{32}P phosphorylated P1 primers were annealed to T1 template at a ratio of 2:1:1. One window gap was filled by DNA polymerase β using photoreactive dCTP analog FAP-dCTP as substrate in primer elongation, and the resulting nick was ligated by T4 DNA ligase. The same primers, T2 template and S4-dUTP were used for preparation of S4-dUMP containing oligonucleotide. To synthesize Antr-dCMP containing strand P3 and P4 were used as primers, T3 as template and Antr-dCTP as substrate in primer elongation by DNA polymerase β. (B) Structures of base-substituted dCTP analogs. (C) Sequences of the damaged DNA model substrates.

3. Results

3.1. Crosslinking of XPC–HR23B to photoreactive DNA

Photoaffinity labeling has been employed to study the interactions between a variety of proteins and their DNA substrates [24]. We have used this technique to display the recognition and binding of damaged DNA by the hetero-dimeric protein complex XPC–HR23B, the primary DNA damage recognition factor. Fig. 1 shows XPC photocrosslinking to 48-mer oligonucleotides, while that of HR23B polypeptide of the hetero-dimeric complex was not detectable. The 48-mer oligonucleotiodes contained photoreactive FAP-dCMP (DNA1–DNA3) or S4-dUMP (DNA4–DNA6) within the DNA strand. Photocrosslinking efficiency decreased in the presence of Mg^{2+} ions. The efficiency was also dependent on the kind of photoreactive dNMP residue, and on the structure of the DNA probes. The most efficient crosslinking was determined in the case of ssDNA (DNA1 and DNA4, Fig. 1, lanes 2, 3 and 11, 12) and for the DNA duplex containing FAP-dCMP residue in one of the strands (DNA2, Fig. 1, lanes 5 and 6). Crosslinking efficiency was much lower for DNA duplex containing S4-dUMP in one of the DNA strands (DNA5, Fig. 1, lanes 14 and 15). The yield in photocrosslinked XPC with the thio group was slightly increased when bulky anthracenyl residue was located in the opposite strand and S4-dUMP was mispaired (DNA6, Fig. 1, lanes 17 and 18 in comparison with lanes 14 and 15). The decreased level of crosslinked adducts in the case of DNA duplex bearing

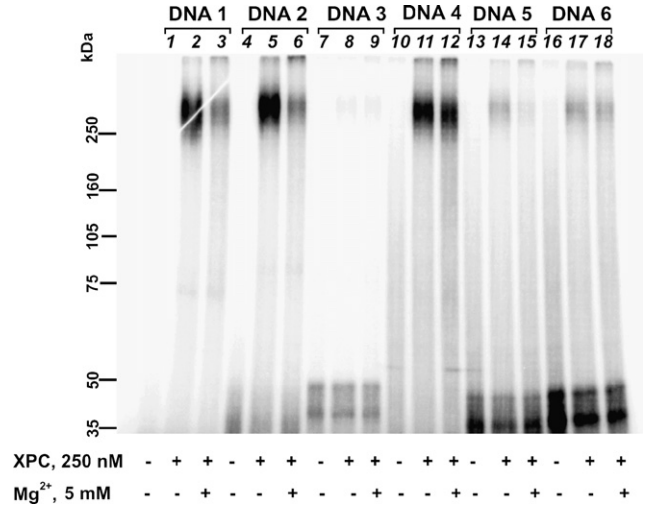

Fig. 1. UV-induced crosslinking of XPC–HR23B to photoreactive DNAs. Indicated amounts of the protein were preincubated with 50 nM single- or double-stranded DNA for 15 min at 37 °C and reaction mixtures (10 μl) were then irradiated with UV-light (312 nm) for 5 min (DNA 1–3) or light of 313–365 nm for 45 min (DNA 4–6) at 4 °C. The photocrosslinked products were separated by SDS–PAGE and visualized by autoradiography. The experiments were reproduced several times and the most representative picture was selected.

thio group in comparison with arylazido group cannot be explained by the lower photoreactivity of 4-thioU group since an approximately equal intensity of XPC crosslinking was found for ssDNA, such as for DNA1 containing FAP-dCMP (Fig. 1, lanes 2 and 3) and DNA4 containing S4-dUMP (Fig. 1, lanes 11 and 12). The explanation is that the 4-thioU group is less distorting the DNA helix and thus represents less damage than the FAP group. The results of similar efficiencies of crosslinking to FAP-dCMP containing 48-mer ssDNA and 48-mer dsDNA (Fig. 1, lanes 2, 3 and 5, 6) are similar to those reported for 60-mer duplexes [17].

The yield of photocrosslinking products is decreased dramatically (more than 20 fold) when the anthracene group is contained in a position opposite to FAP-dCMP (Fig. 1, lanes 8 and 9 in comparison with lanes 5 and 6). By comparison of XPC–HR23B binding to DNA2 and DNA3 using EMSA (results not shown), no visible preference was obvious. This suggested that the difference in the degree of XPC crosslinking reflected a change in the topography of the DNA-protein complex more than a decrease in binding affinity.

The overall result of this section on photocrosslinking of the XPC–HR23B recognition dimer to damaged DNA shows that the method is appropriate to follow the DNA–protein complex formation and that it is sensitive to structural variations at the DNA damage site.

3.2. Crosslinking of RPA and XPA to photoreactive DNA

In addition to the above XPC–HR23B dimer, proteins RPA and XPA are known examples of NER DNA damage recognition proteins. The results of photocrosslinking are shown in Fig. 2. An immediate finding when inspecting the gels is that electrophoretic mobilities of XPA and RPA are retarded after exposure to crosslinking conditions as is exemplified by the comparison of the results for crosslinking with damaged ssDNA and dsDNA. The decreased mobility of the proteins crosslinked to dsDNA is in agreement with the stronger retardation effect of crosslinked dsDNA on mobility than that of ssDNA confirming the fact of a DNA–protein crosslink.

Both RPA and XPA crosslinked to 48-mer ssDNA (DNA1 and DNA4) more efficiently than to 48-mer dsDNA (DNA2, DNA3 and DNA5, DNA6). FAP-dCMP containing DNAs were more efficient probes than the ones containing S4-dUMP. Duplexes DNA5 and DNA6 crosslinked to XPA with extremely low yields (Fig. 2A, lanes 13–18). We only observed bands of DNA–protein adducts after long exposure times (data not shown). RPA crosslinked with DNA5 and DNA6 (Fig. 2B, lanes 13–18), although less effectively than with other DNA probes. In the case of DNA5 only p70 subunit was modified, whereas DNA6 crosslinked also with p32 (Fig. 2B, compare lanes 14 and 15 with lanes 17 and 18), and in sum, the yields of crosslinking adducts with DNA6 were 1.5–2 fold higher. These data are in favor of the assumption that RPA binds

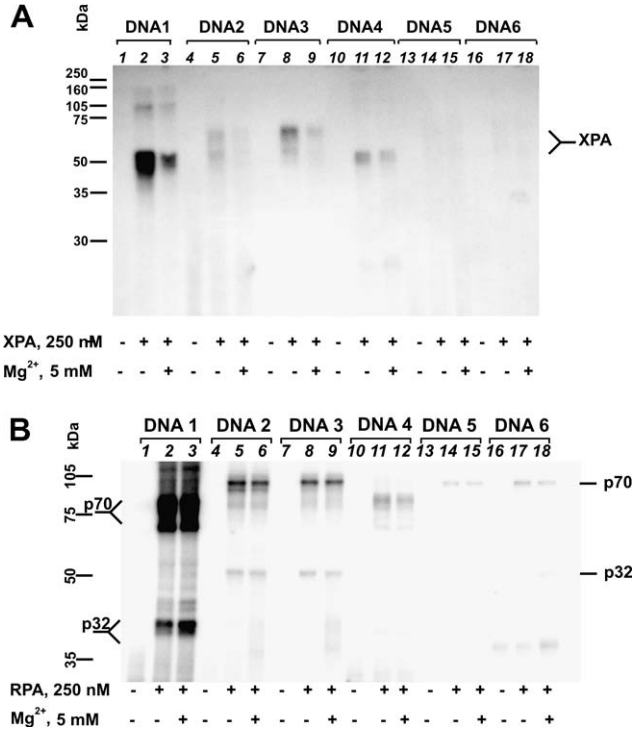

Fig. 2. UV-induced crosslinking of XPA (A) and RPA (B) to photoreactive DNAs. The indicated amounts of RPA or XPA were preincubated with 50 nM single- or double-stranded DNA for 15 min at 37 °C and reaction mixtures (10 μl) were irradiated with UV-light (312 nm) for 5 min (DNAs 1–3) or 313–365 nm for 45 min (DNAs 4–6). The photocrosslinked products were separated by SDS–PAGE and visualized by autoradiography. The experiments were reproduced several times and the most representative picture was selected.

to duplex DNA more tightly than XPA and that XPA interacts with damaged rather than undamaged strand, whereas RPA demonstrates a preference to undamaged strand. DNA3 with the bulky substituents FAP and Antr in both strands crosslinked to XPA more efficiently than DNA2 containing only the FAP residue (Fig. 2A, compare lanes 8 and 9 with lanes 5 and 6). This was opposite to the results when RPA was the crosslinking protein (Fig. 2B, lanes 8, 9 and 5, 6, respectively). Based on the results of EMSA, both XPA and RPA bind with higher affinities to the duplex with one bulky group (DNA2) than to the duplex with two bulky groups (DNA3) (data not shown). The difference in crosslinking efficiency of XPA and RPA with these DNAs suggested an effect of the protein–DNA complex topography, which was different for duplexes with one or two bulky groups.

As in the case of XPC–HR23B, the overall results show that recognition complexes of damaged DNA with protein factors XPA and RPA can be analyzed by photocrosslinking, and that the efficiency of crosslinking reflects topographic differences at the sites of DNA damage.

Numerous reports suggest cooperative interactions of RPA and XPA with damaged DNA [25–27]. To study a mutual interaction of RPA and XPA with damaged DNA we studied the crosslinking of the proteins alone and together with ssDNA (DNA1) and dsDNAs (DNA2 and DNA3) (Fig. 3), these probes having proven to be the most efficient candidates for crosslinking. Fig. 3 shows that XPA does not have a detectable influence on RPA crosslinking (Fig. 3, compare lanes 3 and 5, lanes 8 and 10, lanes 13 and 15). In contrast, RPA influenced XPA crosslinking, depending on the structure of the DNA probe. In the case of ssDNA, the presence of RPA resulted in a reduced level of XPA crosslinking. As can be seen in lane 4, despite 5-fold less concentration of RPA in comparison with XPA, both proteins are modified with about equal intensity. In contrast, in the case of dsDNAs, the effect of RPA on XPA crosslinking was a slight increase, especially noticed for DNA3 (Fig. 3, compare lanes 12 and 14). These effects were reliably reproduced. Overall, the results show that crosslinking efficiencies allow to record interactions between XPA and RPA by virtue of changing the topography of the photoreactive protein–DNA complex at the site of the damage.

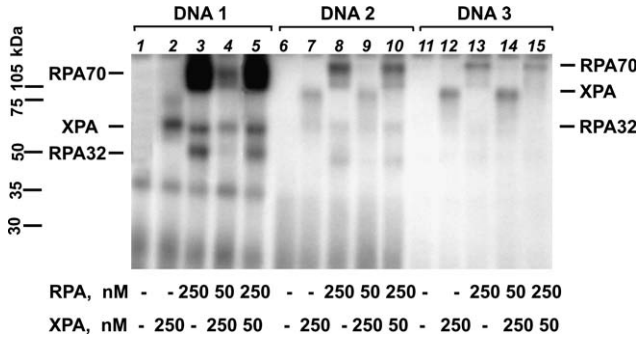

Fig. 3. Mutual interactions of RPA and XPA with damaged DNA. Indicated amounts of RPA and/or XPA were preincubated with 50 nM DNA for 15 min at 37 °C and reaction mixtures (10 μl) were irradiated with UV-light (312 nm) for 5 min at 4 °C. The photocrosslinked products were separated by SDS–PAGE and visualized by autoradiography. Lanes 1–4 : reaction mixtures contained photoreactive DNA duplex with FAP-dCMP residue at ^{32}P-labeled strand. Lanes 5–8 : reaction mixtures contained photoreactive DNA duplex with FAP-dCMP residue at ^{32}P-labeled strand and Antr-dCMP residue at the opposite strand. The experiments were reproduced several times and the most representative picture was selected.

3.3. Binding of XPA and RPA to damaged DNA

To measure the binding of RPA and XPA with model damaged DNA in the absence of photocrosslinking, we followed complex formation between these proteins and DNA3 (duplex, FAP on one strand and Antr juxtapositioned on the other strand) using the gel mobility shift assay (Fig. 4). The concentration of proteins (0.6–4 μM) was in excess of the DNA sample (10 nM). XPA and RPA behaved differently in these binding experiments. When the concentration of XPA was varied, smeared bands were observed, apparently due to instability of the DNA–protein complex (Fig. 4A, lanes 2–5). This was not observed when the concentration of RPA was varied

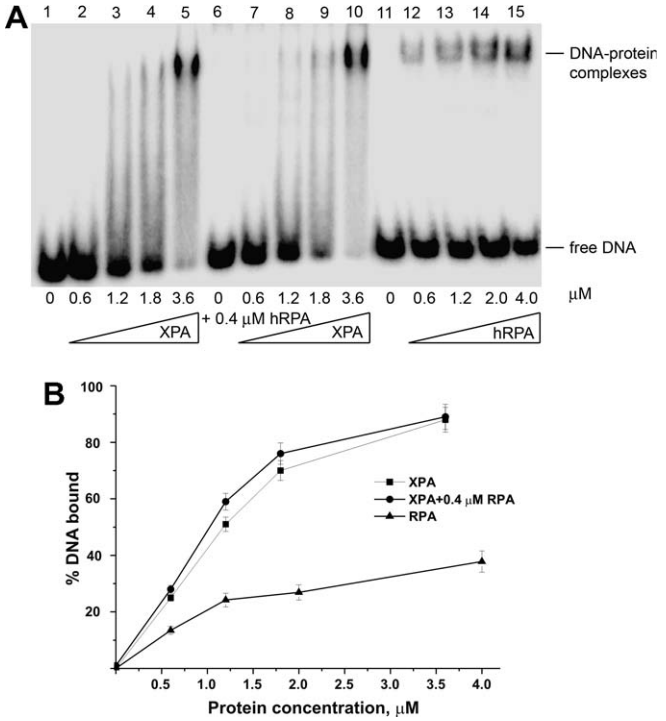

Fig. 4. Binding of XPA and RPA with damaged DNA. DNA duplex (10 nM) containing FAP-dCMP residue at ^{32}P-labeled strand and Antr-dCMP residue at the opposite strand was titrated with increasing amounts of XPA in the absence or presence of 0.4 μM RPA or with increasing amounts of RPA. Binding reactions were subjected to native PAGE as described in Section 2 and analyzed by autoradiography (A). Titration courses were quantitated using BioRad software Quantity One, and the percentage of bound DNA is plotted in (B). Averages and experimental errors were taken from three experiments.

(Fig. 4A, lanes 12–15). The observation was at variance with the higher affinity of XPA for complex formation in comparison with RPA. XPA has been shown to form homodimers [28,29], and the formation of two different kinds of XPA–DNA3 complexes with different electrophoretic mobilities for DNA-monomer and DNA-dimer complexes were assumed to cause the observed smear. To demonstrate an influence of RPA on the binding of XPA to the damaged DNA3, both proteins were present in the reaction mixture (RPA at 0.4 μM while the concentration of XPA was varied). Obviously, a supershift due to complex formation of DNA3 with simultaneously XPA plus RPA was not produced suggesting that the ternary complex was not formed in detectable amounts. The results of the gel shift experiments are in line with those observed by the photocrosslinking experiments, in particular suggesting an effect of the mutual XPA–RPA interaction on the formation of the protein complex with damaged DNA. At these conditions RPA–DNA complexes (Fig. 4A, lane 6) or supershift of XPA–DNA complexes (Fig. 4A, lanes 7–10) were not observed. However titration curves (Fig. 4B) demonstrated a slight increasing of the XPA–DNA binding in the presence of RPA in comparison with XPA alone. This effect correlates with the data obtained in crosslinking experiments (Fig. 3, lanes 12 and 14).

4. Discussion

One of the most astonishing characteristics of the NER pathway is its extraordinarily wide substrate specificity, being able to recognize and repair a large number of structurally unrelated lesions [4]. We synthesized DNA duplexes containing several derivatives of nucleotides, which were recognized by NER proteins as DNA damage sites. Photoreactive nucleotides crosslinked with the proteins allowing to probe for changes in the topography at the site of DNA damage.

In detail, an anthracene-modified deoxycitidine residue at the site of DNA damage in one of the strands and a juxtapositioned photoreactive FAP-dCMP residue on the complementary strand of DNA duplex exert a strong inhibition on XPC–DNA crosslinking to the FAP moiety (Fig. 1). According to gel shift experiments, binding affinities of the XPC–HR23B complex to both doubly modified duplex and dsDNA containing the FAP-damage were similar, and it was concluded that crosslinking efficiency was sensitive to geometry at the site of the DNA–protein complex containing the juxtapositioned damages. Similarly, it has been recently shown by the H. Naegeli laboratory that in comparison to singly damaged duplexes, NER activity in HeLa cell extract toward doubly damaged dsDNA substrates was strongly inhibited [30]. These previous and our results that DNA lesions juxtapositioned in both strands are not recognized effectively by the NER system, probably due to the requirement for XPC–HR23B of an undamaged strand to recruit other NER proteins to form the productive NER complex. The idea of XPC binding via a short open single-stranded DNA stretch opposite to the lesion has also been formulated recently [31]. This idea was directly confirmed with the crystal structure of the yeast XPC orthologue Rad4 bound to 24-mer DNA duplex containing a cyclobutane pyrimidine dimmer (CPD) lesion within a stretch of three nucleotide mismatches [32]. The structure shows interaction of Rad4 with nucleotides of undamaged strand, whereas the two CPD-linked nucleotides become disordered.

The 31 kDa XPA protein is part of the core pre-incision complex of NER and interacts with DNA as well as with other NER protein factors including RPA, TFIIH and ERCC1 [33]. In the absence of XPA, a stable pre-incision complex will not form [12,34] and NER is not observed. In cooperation with RPA, XPA functions as a linchpin in the NER network of interactions [35]. In contrast to XPC, XPA crosslinks with doubly modified duplex efficiently, but it is only marginally crosslinked at DNA lesions containing the thio group (Fig. 2A). These data suggest that XPA interacts with the damaged strand and not with the undamaged one. It was shown earlier that XPA contacts both the damaged and undamaged strands of the duplex DNA [36], and our results are in favor of XPA preference for the damaged strand.

The human RPA is an abundant, hetero-trimeric ssDNA-binding protein complex that is composed of 70-, 32-, and 14-kDa polypeptides. RPA interacts with XPA in NER, and it has been found to specifically bind DNA cisplatin-adducts [37], UV photo-damaged DNA, and acetylaminofluorene adducts [38,39]. Reardon and Sancar [40] have shown crosslinking of RPA to psoralen adducts, whereas neither XPA nor XPC crosslinked to DNA bearing this group. Based on these data, the authors have proposed RPA as a possible candidate of primary damage recognition, at least in the case of such lesions. However these data can be also explained by the assumption, that recognition by XPA and XPC depends on additional features not present in the described psoralen lesion. Our present (Fig. 2B) and earlier photocrosslinking experiments [17,41] show that RPA interacts most efficiently with ssDNA and with damaged DNA bearing a stretch of ssDNA. On this basis, it seems more likely that RPA is recruited in a pre-incision complex depending on TFIIH, namely on DNA next to the lesion already partially unwound by the helicase activities of the XPB and XPD subunits of TFIIH [12,36]. Thus, only after the DNA bubble at the site of the lesion has been opened, RPA binds to the undamaged strand, while XPA binds to the strand bearing the damage site. This positioning of RPA to the undamaged DNA strand [37] establishes a polarity important for the positioning of the nucleases in the pre-incision complex [42,43]. In our experiments the influence of RPA on the XPA crosslinking efficiency with damaged DNA was significantly less than the influence observed in experiments with cisplatin-modified DNA [44]. However, cooperative damage recognition by NER factors is consistent

with numerous experimental data and can be regarded as a crucial question in NER mechanism investigation [15].

5. Conclusion

Photoaffinity labeling technique is one of the promising chemical approaches to study complex and dynamic molecular machines such as DNA repair complexes. Photoreactive DNA imitating NER substrates allow studying direct interaction of key NER proteins with DNA damages. Expansion of this approach should permit the analysis of the sequential assembly of mammalian NER machinery, namely, to study damage recognition and verification by XPC–HR23B, TFIIH and the following assembly of pre-incision complex formed by RPA, XPA, and XPG. Visualization of DNA–protein interactions performed in mammalian NER will provide valuable insight into the molecular basis of this process.

Acknowledgments

This work was supported by grant from HFSP RGP0007/2004-C104, grant from INTAS-SBRAS, project no. 06-1000013-9210, and by the Russian Foundation for Basic Research, project nos. 05-04-48319 and 06-04-48526. The authors are thankful to Prof. Dr. Eggehard Holler for careful reading of the manuscript and useful comments.

References

[1] R.D. Wood, Annu. Rev. Biochem. 65 (1996) 135–167.
[2] A. Sancar, Annu. Rev. Biochem. 65 (1996) 43–81.
[3] O.D. Schärer, Angew. Chem. Int. Ed. Engl. 42 (2003) 2946–2974.
[4] L.C. Gillet, O.D. Schärer, Chem. Rev. 106 (2006) 253–276.
[5] V.A. Bohr, C.A. Smith, D.S. Okumoto, P.C. Hanawalt, Cell 40 (1985) 359–369.
[6] N. Buschta-Hedayat, T. Buterin, M.T. Hess, M. Missura, H. Naegeli, Proc. Natl. Acad. Sci. USA 96 (1999) 6090–6095.
[7] K. Sugasawa, T. Okamoto, Y. Shimizu, C. Masutani, S. Iwai, F. Hanaoka, Genes Dev. 15 (2001) 507–521.
[8] K. Sugasawa, J.M. Ng, C. Masutani, S. Iwai, P.J. van der Spek, A.P. Eker, F. Hanaoka, D. Bootsma, J.H. Hoeijmakers, Mol. Cell 2 (1998) 223–232.
[9] M. Volker, M.J. Mone, P. Karmakar, A. van Hoffen, W. Schul, W. Vermeulen, J.H. Hoeijmakers, R. van Driel, A.A. van Zeeland, L.H. Mullenders, Mol. Cell 8 (2001) 213–224.
[10] M. Araki, C. Masutani, M. Takemura, A. Uchida, K. Sugasawa, J. Kondoh, Y. Ohkuma, F. Hanaoka, J. Biol. Chem. 276 (2001) 18665–18672.
[11] M. Yokoi, C. Masutani, T. Maekawa, K. Sugasawa, Y. Ohkuma, F. Hanaoka, J. Biol. Chem. 275 (2000) 9870–9875.
[12] E. Evans, J.G. Moggs, J.R. Hwang, J.M. Egly, R.D. Wood, EMBO J. 16 (1997) 6559–6573.
[13] S.J. Araujo, E.A. Nigg, R.D. Wood, Mol. Cell. Biol. 21 (2001) 2281–2291.
[14] J.T. Reardon, A. Sancar, Genes Dev. 17 (2003) 2539–2551.
[15] K.J. Kesseler, W.K. Kaufmann, J.T. Reardon, T.C. Elston, A. Sancar, J. Theor. Biol. 249 (2007) 361–375.
[16] M.J. Dellavecchia, D.L. Croteau, M. Skorvaga, S.V. Dezhurov, O.I. Lavrik, B. Van Houten, J. Biol. Chem. 279 (2004) 45245–45256.
[17] E.A. Maltseva, N.I. Rechkunova, L.C. Gillet, I.O. Petruseva, O.D. Schärer, O.I. Lavrik, Biochem. Biophys. Acta 1770 (2007) 781–789.
[18] S.V. Dezhurov, S.N. Khodyreva, E.S. Plekhanova, O.I. Lavrik, Bioconjug. Chem. 16 (2005) 215–222.
[19] L.A. Henricksen, C.B. Umbricht, M.S. Wold, J. Biol. Chem. 269 (1994) 11121–11132.
[20] D. Batty, V. Rapic'-Otrin, A.S. Levine, R.D. Wood, J. Mol. Biol. 300 (2000) 275–290.
[21] W.A. Beard, S.H. Wilson, Methods Enzymol. 262 (1995) 98–107.
[22] J. Sambrook, E.F. Fritsch, T. Maniatis, Molecular Cloning: A Laboratory Manual, second ed., Cold Spring Harbor Laboratory, Cold Spring Harbor, NY, 1989.
[23] U.K. Laemmli, Nature 227 (1970) 680–685.
[24] S.N. Khodyreva, O.I. Lavrik, Curr. Med. Chem. 12 (2005) 641–655.
[25] T. Hey, G. Lipps, G. Krauss, Biochemistry 40 (2001) 2901–2910.
[26] L. Li, X. Lu, C.A. Peterson, R.J. Legerski, Mol. Cell. Biol. 15 (1995) 5396–5402.
[27] M. Wang, A. Mahrenholz, S.-H. Lee, Biochemistry 39 (2000) 6433–6439.
[28] Z.G. Yang, Y. Liu, L.Y. Mao, J.T. Zhang, Y. Zou, Biochemistry 41 (2002) 13012–13020.
[29] Y. Liu, Y. Liu, Z. Yang, C. Utzat, G. Wang, A.K. Basu, Y. Zou, Biochemistry 44 (2005) 7361–7368.
[30] T. Buterin, C. Meyer, B. Giese, H. Naegeli, Chem. Biol. 12 (2005) 913–922.
[31] O. Maillard, S. Solyom, H. Naegeli, PLoS Biol. 5 (2007) e79.
[32] J.-H. Min, N.P. Pavletich, Nature 449 (2007) 570–575.
[33] M. Saijo, I. Kuraoka, C. Masutani, F. Hanaoka, K. Tanaka, Nucleic Acids Res. 24 (1996) 4719–4724.
[34] D. Mu, M. Wakasugi, D.S. Hsu, A. Sancar, J. Biol. Chem. 272 (1997) 28971–28979.
[35] I.I. Hermanson-Miller, J.J. Turchi, Biochemistry 41 (2002) 2402–2408.
[36] C.J. Park, B.S. Choi, FEBS J. 273 (2006) 1600–1608.
[37] C.K. Clugston, K. McLaughlin, M.K. Kenny, R. Brown, Cancer Res. 52 (1992) 6375–6379.
[38] Z. He, L.A. Henricksen, M.S. Wold, C.J. Ingles, Nature 374 (1995) 566–569.
[39] J.L. Burns, S.N. Guzder, P. Sung, S. Prakash, L. Prakash, J. Biol. Chem. 271 (1996) 11607–11610.
[40] J.T. Reardon, A. Sancar, Mol. Cell. Biol. 22 (2002) 5938–5945.
[41] E.A. Maltseva, N.I. Rechkunova, I.O. Petruseva, V.N. Silnikov, W. Vermeulen, O.I. Lavrik, Biochemistry (Moscow) 71 (2006) 270–278.
[42] W.L. de Laat, E. Appeldoorn, K. Sugasawa, E. Weterings, N.G. Jaspers, J.H. Hoeijmakers, Genes Dev. 12 (1998) 2598–2609.
[43] D.M. Kolpashchikov, S.N. Khodyreva, D.Y. Khlimankov, M.S. Wold, A. Favre, O.I. Lavrik, Nucleic Acids Res. 29 (2001) 373–379.
[44] U. Schweizer, T. Hey, G. Lipps, G. Krauss, Nucleic Acids Res. 27 (1999) 3183–3189.